

See discussions, stats, and author profiles for this publication at: <https://www.researchgate.net/publication/24417981>

# Mechanism of Lysophosphatidic Acid-Induced Amyloid Fibril Formation of $\beta$ 2 -Microglobulin in Vitro under Physiological Conditions

ARTICLE in BIOCHEMISTRY · JUNE 2009

Impact Factor: 3.02 · DOI: 10.1021/bi900356r · Source: PubMed

CITATIONS

22

READS

48

12 AUTHORS, INCLUDING:



Janos Kovács

Eötvös Loránd University

99 PUBLICATIONS 1,893 CITATIONS

SEE PROFILE



Judit Fidy

Semmelweis University

127 PUBLICATIONS 1,623 CITATIONS

SEE PROFILE



Karoly Liliom

Hungarian Academy of Sciences

53 PUBLICATIONS 1,686 CITATIONS

SEE PROFILE

## Mechanism of Lysophosphatidic Acid-Induced Amyloid Fibril Formation of $\beta_2$ -Microglobulin *in Vitro* under Physiological Conditions<sup>†</sup>

Henriett Pál-Gábor,<sup>‡,§</sup> Linda Gombos,<sup>‡</sup> András Micsonai,<sup>‡</sup> Erika Kovács,<sup>§</sup> Éva Petrik,<sup>‡</sup> János Kovács,<sup>||</sup> László Gráf,<sup>‡</sup> Judit Fidy,<sup>⊥</sup> Hironobu Naiki,<sup>#</sup> Yuji Goto,<sup>△</sup> Károly Liliom,<sup>§,◇</sup> and József Kardos<sup>\*,‡,◇</sup>

<sup>‡</sup>Department of Biochemistry and <sup>||</sup>Department of Anatomy, Cell and Developmental Biology, Institute of Biology, Eötvös Loránd University, Budapest, H-1117 Hungary, <sup>§</sup>Institute of Enzymology, Hungarian Academy of Sciences, Budapest, H-1113 Hungary, <sup>⊥</sup>Institute of Biophysics and Research Group for Biomembranes HAS, Semmelweis Medical University, Budapest, H-1088 Hungary, <sup>#</sup>Division of Molecular Pathology, Department of Pathological Sciences, Faculty of Medical Sciences, University of Fukui and CREST, Japan Science and Technology Agency, Fukui 910-1193, Japan, and <sup>△</sup>Institute for Protein Research, Osaka University and CREST, Japan Science and Technology Agency, Osaka 565-0871, Japan <sup>◇</sup>Senior coauthors

Received March 2, 2009; Revised Manuscript Received May 7, 2009

**ABSTRACT:**  $\beta_2$ -microglobulin- ( $\beta_2$ m-) based fibril deposition is the key symptom in dialysis-related amyloidosis.  $\beta_2$ m readily forms amyloid fibrils *in vitro* at pH 2.5. However, it is not well understood which factors promote this process *in vivo*, because  $\beta_2$ m cannot polymerize at neutral pH without additives even at elevated concentration. Here we show that lysophosphatidic acid (LPA), an *in vivo* occurring lysophospholipid mediator, promotes amyloid formation under physiological conditions through a complex mechanism. In the presence of LPA, at and above its critical micelle concentration, native  $\beta_2$ m became sensitive to limited proteolytic digestion, indicating increased conformational flexibility. Isothermal titration calorimetry indicates that  $\beta_2$ m exhibits high affinity for LPA. Fluorescence and CD spectroscopy, as well as calorimetry, showed that LPA destabilizes the structure of monomeric  $\beta_2$ m inducing a partially unfolded form. This intermediate is capable of fibril extension in a nucleation-dependent manner. Our findings also indicate that the molecular organization of fibrils formed under physiological conditions differs from that of fibrils formed at pH 2.5. Fibrils grown in the presence of LPA depolymerize very slowly in the absence of LPA; moreover, LPA stabilizes the fibrils even below its critical micelle concentration. Neither the amyloidogenic nor the fibril-stabilizing effects of LPA were mimicked by its structural and functional lysophospholipid analogues, showing its selectivity. On the basis of our findings and the observed increase in blood LPA levels in dialysis patients, we suggest that the interaction of LPA with  $\beta_2$ m might contribute to the pathomechanism of dialysis-related amyloidosis.

The development of amyloid disorders in the human body, such as Alzheimer's and Parkinson's diseases, or dialysis-related amyloidosis have been shown to be accompanied by an elevated concentration of the pathogenic protein (1, 2). Although increased protein concentration seems to be a prerequisite for amyloid formation, it is not sufficient by itself to explain the progress and symptoms of the diseases. A great interest has

emerged recently in searching for specific molecules that may affect the malicious aggregation and amyloid propagation of disease-related proteins.

$\beta_2$ -Microglobulin ( $\beta_2$ m)<sup>1</sup> is the light chain of the type I major histocompatibility complex. After dissociating from the complex, it appears in monomeric form in blood. In patients undergoing long-term hemodialysis, an elevated level of  $\beta_2$ m was observed due to insufficient clearance of the protein, accompanied by amyloid deposition in the osteoarticular system (3).  $\beta_2$ m is a 99-residue protein which has a native, monomeric structure at pH 7.5, composed of two  $\beta$ -sheets connected by a disulfide bridge. At pH 2.5,  $\beta_2$ m is acid denatured and readily forms amyloid fibrils in a nucleation-dependent manner *in vitro* (4–8). However,  $\beta_2$ m forms no fibrils at neutral pH, even at protein concentrations 1000-fold higher than the physiological one (9), indicating that specific factors facilitate the amyloid formation of  $\beta_2$ m *in vivo*. Numerous studies reported the possible role of glycosaminoglycans (10–13), apolipoprotein E (14), serum amyloid protein (15), and collagen (13, 16–18) in fibrillogenesis of  $\beta_2$ m. *In vitro*, amyloid formation of  $\beta_2$ m at neutral pH occurs in the presence of

<sup>†</sup>J.K. is a fellow of the Bolyai János Scholarship of the Hungarian Academy of Sciences and Öveges József Program of NKTH. L.G. was supported by a Deák Ferenc Fellowship. This work was supported by the Hungarian National Science Foundation (OTKA 61501, 68464, and TS049812) and the Medical Research Council (ETT 555/2006). The international collaboration was also supported by Hungarian T&T and the Institute for Protein Research, Osaka University.

\*Correspondence should be addressed to this author: phone, +36 1209 0555/1795; fax, +36 1381 2172; e-mail, kardos@elte.hu.

Abbreviations:  $\beta_2$ m,  $\beta_2$ -microglobulin; CMC, critical micelle concentration; DRA, dialysis-related amyloidosis; DSC, differential scanning calorimetry; ITC, isothermal titration calorimetry; LPA, lysophosphatidic acid; LPC, lysophosphatidylcholine; SDS, sodium dodecyl sulfate; S1P, sphingosine 1-phosphate; SPC, sphingosylphosphorylcholine; ThT, thioflavin T.

copper ions (19–21) or requires the addition of seeds (e.g., seeds prepared from fibrils preformed at pH 2.5 and stabilized by heparin or other additives) in the presence of trifluoroethanol or SDS (12, 22).

The nucleation-dependent amyloid formation of  $\beta$ 2m in the presence of SDS has been characterized in detail (7, 22, 23). Very recently, Ookoshi et al. have shown that some lysophospholipids, especially lysophosphatidic acid (LPA), also induce the formation of  $\beta$ 2m amyloid fibrils at neutral pH (24). LPA is an amphiphilic molecule with a negatively charged headgroup and a hydrophobic tail of one alkyl chain; thus it is structurally similar to SDS. It is present in numerous biological fluids including blood (25). LPA is a widespread lysophospholipid mediator with a plethora of biological effects. In cellular physiology, LPA promotes proliferation, survival, motility, and differentiation of cells (26). Furthermore, it plays important roles in the cardiovascular and reproductive biology and in the development of the nervous system. On the other hand, LPA takes part in different pathological processes such as cancer and atherosclerosis (27, 28).

In this work, we studied the mechanism of LPA-induced amyloid fibril formation of  $\beta$ 2m at physiological pH, temperature, and ionic strength. We found that micellar LPA destabilizes the structure of monomeric  $\beta$ 2m, promotes seed-dependent amyloid formation, and stabilizes preformed amyloid fibrils. Physiologically relevant and structurally related lysophospholipids showed no significant effects, underlining the specificity of the  $\beta$ 2m–LPA interaction.

## EXPERIMENTAL PROCEDURES

**Materials.** Lipids were purchased from Avanti Polar Lipids (Alabaster, AL), and other chemicals were from Sigma-Aldrich. Recombinant  $\beta$ 2m was expressed in *Escherichia coli* and purified as described previously (21, 29).

**Polymerization Reaction under Physiological Conditions.** Seeds were prepared by sonication of 100  $\mu$ L aliquots from amyloid fibril solutions using a Microson sonicator (Misonix, Farmingdale, NY) at intensity level 2, with 50 1-s pulses on ice. In the first polymerization cycle, seeds grown at pH 2.5 were used at a concentration of 20  $\mu$ g/mL for inducing fibril extension in the presence of LPA. For subsequent cycles, seeds were obtained from the previous cycle. Seeds obtained from the fifth cycle were used for the experiments. The mixtures were incubated at 37 °C without agitation for 1–7 days. Fibril growth was monitored by thioflavin T (ThT) fluorescence. The reaction mixture contained 0.1 mg/mL  $\beta$ 2m, 10  $\mu$ g/mL seeds, 50 mM sodium phosphate or HEPES buffer (pH 7.5), 100 mM NaCl, and various concentrations of LPA in the range of 50–700  $\mu$ M. Experiments in the presence of lipids other than LPA were carried out at 500  $\mu$ M lipid concentration. The required quantities of lipids were dried from 10 mM methanolic stock solutions into test tubes and redissolved in the reaction mixture by vigorous vortexing and sonication. S1P was directly diluted into the reaction buffer from 10 mM methanolic stock solution.

**Thioflavin T Fluorescence Measurements.** Five microliter aliquots were taken from the samples and mixed with 1.0 mL of 5  $\mu$ M ThT in 50 mM glycine and 100 mM NaCl, pH 8.5 (30). Fluorescence intensity of ThT was monitored at 485 nm with excitation at 445 nm at 25 °C, using a Fluoromax instrument (SPEx Industries, Edison, NJ). Excitation and emission bandwidths were set to 5 and 10 nm, respectively.

**Circular Dichroism Spectroscopy.** CD measurements were carried out on a Jasco J-720 spectropolarimeter (Japan Spectroscopic Co., Tokyo, Japan). A cylindrical water-jacketed quartz cell of 0.1 cm path length was used. CD spectra in the range of 200–240 nm were recorded at a scanning speed of 10 nm/min in continuous mode using a bandwidth of 1 nm at a temperature of 37 °C. The secondary structure composition of  $\beta$ 2m monomers and amyloid fibrils was examined by the Dicroprot (31) and GlobalWorks (Olis Inc., Bogart, GA) software packages.

**Limited Proteolysis by Chymotrypsin.**  $\beta$ 2m (0.2 mg/mL) was incubated in either 50 mM sodium phosphate or 50 mM HEPES buffer, pH 7.5, containing 100 mM NaCl at 37 °C in the absence or presence of various concentrations of LPA and LPC (25–300  $\mu$ M). After 1 h preincubation, bovine  $\alpha$ -chymotrypsin (Worthington Biochemical Co., Lakewood, NJ) was added to the reaction mixture at 1:100 enzyme to substrate molar ratio. Proteolytic digestion was allowed to proceed for 30 min at 37 °C and stopped by the addition of 2 $\times$  reducing SDS sample buffer and heating at 95 °C for 5 min. Proteolytic fragments were separated by 16.5% SDS–PAGE in Tris/Tricine buffer (32, 33). Gels were fixed in 50% methanol and 9% acetic acid for 30 min and stained with Brilliant Blue G in 5% methanol and 7% acetic acid overnight.

**Electron Microscopy.** Samples were applied directly to 300-mesh Formvar/carbon-coated copper grids, allowed to adhere for 1 min, and stained for 40 s with 1% uranyl acetate. Grids were examined by a JEOL 100 CX II transmission electron microscope (JEOL Ltd., Tokyo, Japan) at an accelerating voltage of 60 kV.

**Differential Scanning Calorimetry.** Experiments were carried out on a VP-DSC instrument (MicroCal Inc., MA). Protein solutions (0.2 mg/mL) were examined in the presence of various concentrations of different lipids in 50 mM sodium phosphate and 100 mM NaCl, pH 7.5. Thermal unfolding profiles were analyzed by Origin 7.0 for DSC (MicroCal Inc., MA).

**Heat-induced Dissociation of  $\beta$ 2m Fibrils at pH 2.5.** Amyloid fibrils were grown at pH 2.5 in 50 mM sodium citrate buffer and 100 mM NaCl. Samples contained 0.1 mg/mL fibrils in the same buffer and 500  $\mu$ M different lipids or SDS. Twenty microliter aliquots were incubated in 200  $\mu$ L thin-walled PCR tubes, for better heat transfer, at various temperatures in the 25–99 °C range using a Hybaid PCR Sprint thermal cycler (Mandel Scientific, Canada). After 5 min, the reactions were stopped by placing the tubes on ice. Fibril dissociation was monitored by the remaining ThT fluorescence.

**Depolymerization of  $\beta$ 2m Fibrils at pH 7.5.** The tenth generation of fibrils were grown as described above in the presence of 300  $\mu$ M LPA. The lipid was removed by repeated cycles of centrifugation and washing with LPA-free buffer. Fibrils were resuspended at a concentration of 0.05 mg/mL in buffer containing various concentrations of LPA in the range of 5–300  $\mu$ M and in LPA-free buffer for reference and incubated at 37 °C for up to 2 months. The amount of fibrils was monitored by ThT fluorescence.

**Isothermal Titration Calorimetry.** Critical micelle concentrations (CMC) of LPA and LPC were determined by isothermal titration calorimetry (ITC) using a VP-ITC instrument (MicroCal Inc., MA) at 37 °C in a buffer containing 50 mM sodium phosphate and 100 mM NaCl at pH 7.5, similarly to Li et al. (34). Micellar solutions (2–10  $\mu$ L) of 1 mM LPA or 500  $\mu$ M LPC were injected repeatedly into the calorimeter cell containing only the buffer solution at the beginning. Reaction heat was corrected

with appropriate buffer–buffer measurements. The CMC value was defined as the lipid concentration in the cell that corresponds to a heat effect less than 5% of the initial maximal value.

Interaction of native, monomeric  $\beta 2m$  with LPA was also examined by ITC. Ten microliter aliquots of  $\beta 2m$  at a concentration of 470  $\mu M$  in a buffer of 50 mM sodium phosphate and 100 mM NaCl, pH 7.5, were injected into the ITC cell containing 300  $\mu M$  LPA in the same buffer. A time interval of 1 h was applied between injections. Titration curves were analyzed, and the binding energetics were characterized using the Origin software provided by MicroCal.

## RESULTS

At neutral pH,  $\beta 2m$  is not capable of amyloid formation without additives even in the presence of fibril seeds (14, 22, 23, 35). Moreover, fibrils formed at low pH will dissociate at neutral pH (14, 23). We studied the effect of LPA on the fibril formation of  $\beta 2m$  at pH 7.5 in either sodium phosphate or HEPES buffers at 37 °C. LPA is an acronym for a set of glycerophospholipids in which the apolar hydrocarbon chain can differ in length and saturation. Additionally, it can be coupled to the glycerol backbone by an ester, ether, or vinyl–ether bond. Naturally occurring LPA is usually a mixture of these varieties. In the majority of studies, oleoyl-LPA evokes a similar response to the natural mixture, so it is considered as the model compound for the biological actions of LPA. Thus, we used oleoyl-LPA throughout the present study to investigate the biologically relevant effects of LPA on the structure and amyloidogenicity of  $\beta 2m$ . Moreover, in the comprehensive work of Ookoshi et al. (24), oleoyl LPA was proven to be one of the lysophospholipids that effectively induced elongation of seeds prepared from fibrils grown in the presence of SDS at neutral pH.

**Fibril Formation in the Presence of LPA under Physiological Conditions.** We studied the effect of LPA on the fibril formation of  $\beta 2m$  at pH 7.5 by ThT fluorescence (Figure 1A).  $\beta 2m$  monomers were incubated in the presence of 500  $\mu M$  oleoyllysophosphatidic acid (LPA), oleoyllysophosphatidylcholine (LPC), sphingosine 1-phosphate (S1P), sphingosylphosphorylcholine (SPC), or sodium dodecyl sulfate (SDS) for 24 h (see the structures in Figure 1B). Polymerization was induced by seeds prepared from amyloid fibrils grown at pH 2.5. In the presence of LPA and SDS, a significant increase in ThT fluorescence intensity was observed, indicating the aggregation of  $\beta 2m$ . The other lipids exerted no detectable increase in fluorescence intensity, meaning they do not induce polymerization. However, the initial high level of ThT fluorescence first decreased fast in the presence of all lipids, indicating a depolymerization of the seeds. In the presence of SDS this effect was much less pronounced (Figure 1A inset), suggesting a different stabilizing effect of SDS on amyloid fibrils.

**Fibril Formation as a Function of LPA Concentration and Incubation Time.**  $\beta 2m$  monomers were incubated in the presence of fibril seeds and various concentrations of LPA at pH 7.5. For these experiments seeds were prepared from the fifth generation of fibrils grown at pH 7.5 in the presence of 300  $\mu M$  LPA. We found that the kinetics of fibril growth depended on LPA concentration (Figure 2). Fibril growth was unambiguously detectable at 100  $\mu M$  LPA concentration. The growth rate and ThT fluorescence intensity exhibited maximal values around 300  $\mu M$  LPA. Above this concentration both the growth rate and maximum fluorescence values decreased. Utilizing seeds grown at

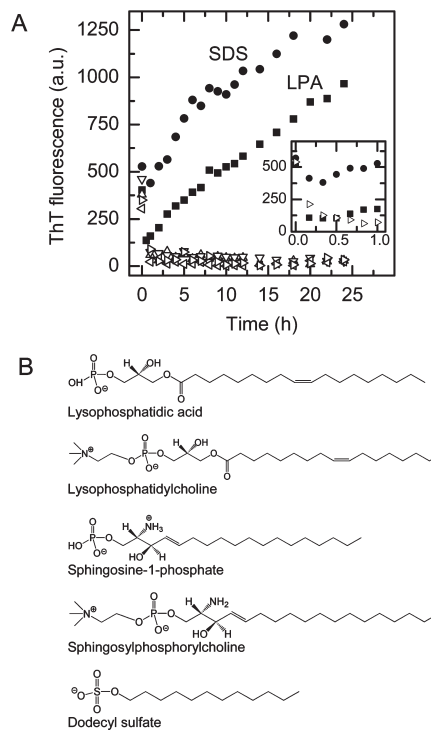


FIGURE 1: Effect of LPA and related analogues on the fibril formation of  $\beta 2m$  at pH 7.5. Fibril growth was monitored by ThT fluorescence. (A)  $\beta 2m$  monomers at a concentration of 0.1 mg/mL were incubated in the presence of 500  $\mu M$  LPA (■), LPC (△), S1P (left-pointing triangle), SPC (▽), and SDS (●) in 50 mM sodium phosphate and 100 mM NaCl, pH 7.5 at 37 °C. Samples were inoculated with 20  $\mu g/mL$  fibril seeds prepared from fibrils formed at pH 2.5. Reaction mixtures were incubated for 24 h at 37 °C. For comparison, ThT fluorescence of  $\beta 2m$  was examined in the absence of additives under the same conditions (right-pointing triangle). The first hour of the progress curves for SDS, LPA, and the lipid-free control are depicted in the inset of panel A. Typical experiments of five determinations are shown. The experimental errors were less than 10%. (B) Structures of the additives used in the experiments (LPA, LPC, S1P, SPC, and SDS).

different LPA concentrations led to similar results, exhibiting growth maxima around 300  $\mu M$  LPA (data not shown).

**Fibril Morphology Studied by Electron Microscopy.** The morphology of  $\beta 2m$  aggregates in samples exhibiting high ThT fluorescence intensity was studied by electron microscopy. Figure 3 shows electron micrographs of fibrils formed in a seeded reaction in the presence of 300  $\mu M$  LPA at pH 7.5. The fibrils consisted of several protofibrils and showed twisted morphology. Generally, the thickness of fibrils was proven to be in the range of 20–50 nm at pH 7.5, with a few exceptions showing 8–10 nm diameter. For fibrils formed at pH 2.5, a smaller thickness of 5–15 nm has been reported (8).

**Effect of LPA on the Secondary Structure of Native  $\beta 2m$  Studied by CD Spectroscopy.** Figure 4 shows alterations in the secondary structure of native, monomeric  $\beta 2m$  upon interaction with various concentrations of LPA at pH 7.5. Far-UV CD spectra were recorded every 5 min for 2 h, and a final spectrum was recorded after 24 h. Above 150  $\mu M$  LPA concentration, significant changes in the CD spectra were observed, indicating destabilization of the native conformation with a decrease in the extent of ordered secondary structure (Figure 4D–H). The spectral changes were fully completed within 1–2 h with amplitudes depending on LPA concentration. Measurements at 24 h incubation showed no additional changes compared to the 2 h



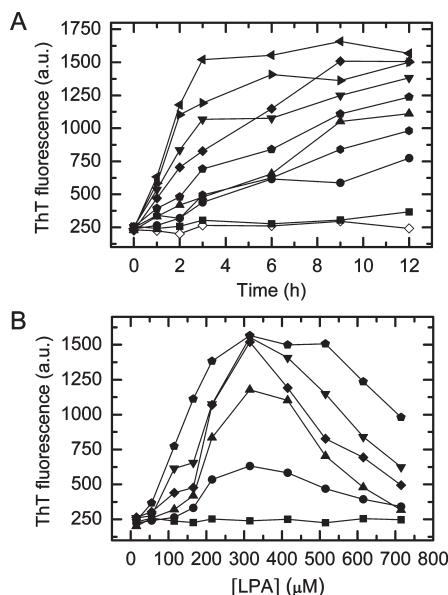


FIGURE 2: Amyloid fibril formation of  $\beta 2m$  as a function of LPA concentration at physiological pH.  $\beta 2m$  monomer solutions containing different concentrations of LPA were inoculated with seeds prepared from the fifth generation of fibrils formed at pH 7.5 in the presence of 300  $\mu M$  LPA. The samples contained 0.1 mg/mL  $\beta 2m$  monomer and 10  $\mu g/mL$  seeds in 50 mM sodium phosphate and 100 mM NaCl, pH 7.5, and were incubated at 37 °C. As a reference, a sample without lipid was also examined. Fibril growth was monitored by ThT fluorescence. The data set of amyloid fibril formation is shown as a function of incubation time (A) in the presence of 0  $\mu M$  ( $\diamond$ ), 50  $\mu M$  ( $\blacksquare$ ), 100  $\mu M$  ( $\bullet$ ), 150  $\mu M$  ( $\blacktriangle$ ), 200  $\mu M$  ( $\blacktriangledown$ ), 300  $\mu M$  (left-pointing triangle), 400  $\mu M$  (right-pointing triangle), 500  $\mu M$  ( $\blacklozenge$ ), 600  $\mu M$  (solid  $\circ$ ), and 700  $\mu M$  LPA ( $\bullet$ ), as well as of LPA concentration (B) at 0 h ( $\blacksquare$ ), 1 h ( $\bullet$ ), 2 h ( $\blacktriangle$ ), 3 h ( $\diamond$ ), 6 h ( $\blacktriangledown$ ), and 12 h (solid  $\circ$ ). A typical experiment of three determinations is shown. The experimental error was less than 10%.

time points (Figure 4A–H, dotted lines). In the presence of 500  $\mu M$  LPC, no change in the secondary structure was detected similarly to the lipid-free control (Figure 4A,B). Figure 4I illustrates the kinetics of  $\beta 2m$ –LPA interaction as a function of LPA concentration by monitoring the ellipticity change at 205 nm. The rate of conformational change is accelerated at higher LPA concentrations. At 700  $\mu M$  LPA, the reaction is completed within 30 min. We estimated the secondary structure content of the different forms of monomeric  $\beta 2m$  using the algorithms of SELCON3 (36), VARSLC (37), CDSSTR (38), CONTIN (39), CONTINLL (40, 41), and K2D (42). The results are presented in Supporting Information Table 1. Although the different prediction algorithms provided different values, we could observe clear tendencies in the secondary structure changes. At 300  $\mu M$  LPA, a decrease in  $\beta$ -sheet and an appearance of  $\alpha$ -helix were observed compared to the native  $\beta 2m$ . At 500  $\mu M$  LPA, a further decrease in  $\beta$ -sheet content was detected with a possible additional small increase of the  $\alpha$ -helical structure. The changes in the other secondary structural elements were not unambiguously estimated; however, some of the algorithms suggested an increase in the unordered structure.

**Cross-Linking of LPA-Destabilized  $\beta 2m$ .** Native  $\beta 2m$  is a monomeric protein. Cross-linking experiments were carried out to verify if  $\beta 2m$  remains monomeric upon partial unfolding from the native state induced by LPA. Dithiobis(succinimidyl propionate) (DTSP), an amine-reactive cross-linker, was used to stabilize the dimers present, if any, in samples incubated with LPA. The possible dimerization of  $\beta 2m$  was examined by

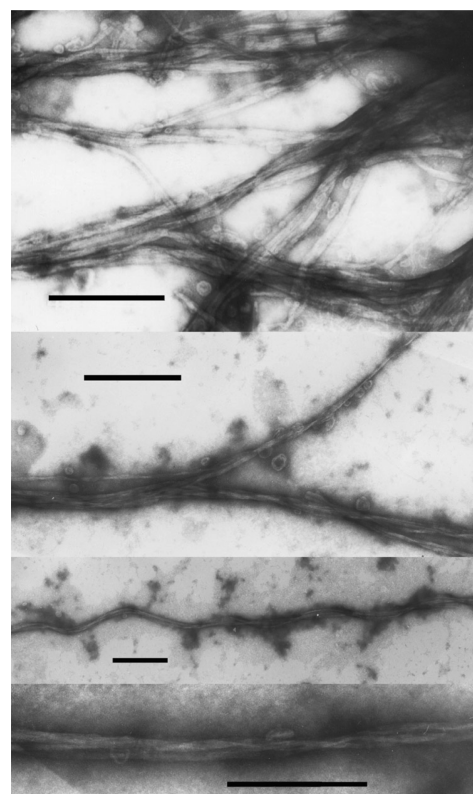


FIGURE 3: Electron microscopy of  $\beta 2m$  fibrils formed in the presence of LPA. Amyloid fibrils were formed by incubation of 0.1 mg/mL  $\beta 2m$  with 300  $\mu M$  LPA in 50 mM sodium phosphate and 100 mM NaCl, pH 7.5, for 24 h at 37 °C. Mature fibrils were stained with 1% uranyl acetate and examined by transmission electron microscopy. Scale bars represent 300 nm. The typical morphology is a bundle of numerous fibrils twisted around one another.

SDS–PAGE under nonreducing conditions. The results showed no detectable dimerization in the presence of LPA under the conditions used in the present work as explained and presented in detail in Supporting Information Figure 2.

**CD Spectroscopy of Amyloid Fibrils Formed in the Presence of LPA.** Figure 5 shows amyloid fibril formation of  $\beta 2m$  in the presence of LPA using amyloid seeds grown at pH 7.5. Before the seed-induced fibril formation,  $\beta 2m$  monomers were preincubated for 2 h at 37 °C in the presence of either 300 or 500  $\mu M$  LPA. After addition of seeds, CD spectra were recorded at various incubation times. Consistently with ThT fluorescence measurements, fibril generation was detected only in the presence of both LPA and fibril seeds. After 48 h, intensive amyloid-like CD spectra of high  $\beta$ -sheet content with single negative maxima at 221 and 218 nm were observed at 300 and 500  $\mu M$  LPA concentrations, respectively. Note the isodichroic point in the case of 300  $\mu M$  LPA, implicating that two conformational species of  $\beta 2m$  are present in the solution, i.e., amyloid fibrils and partially unfolded monomers. Figure 5C shows the representative CD spectra of the different monomeric and fibrillar forms of  $\beta 2m$ . Fibril samples showed precipitates of associated fibrils after 1 week of incubation. To resuspend and homogenize these samples, we applied slight ultrasonication. This process increased the amplitude of the CD spectra significantly, indicating that the larger aggregates of fibrils are not detectable by CD spectroscopy.

**Limited Proteolysis of Monomeric  $\beta 2m$  in the Presence of LPA.**  $\beta 2m$  was subjected to limited proteolysis by chymotrypsin at pH 7.5 to determine the lowest LPA concentration that

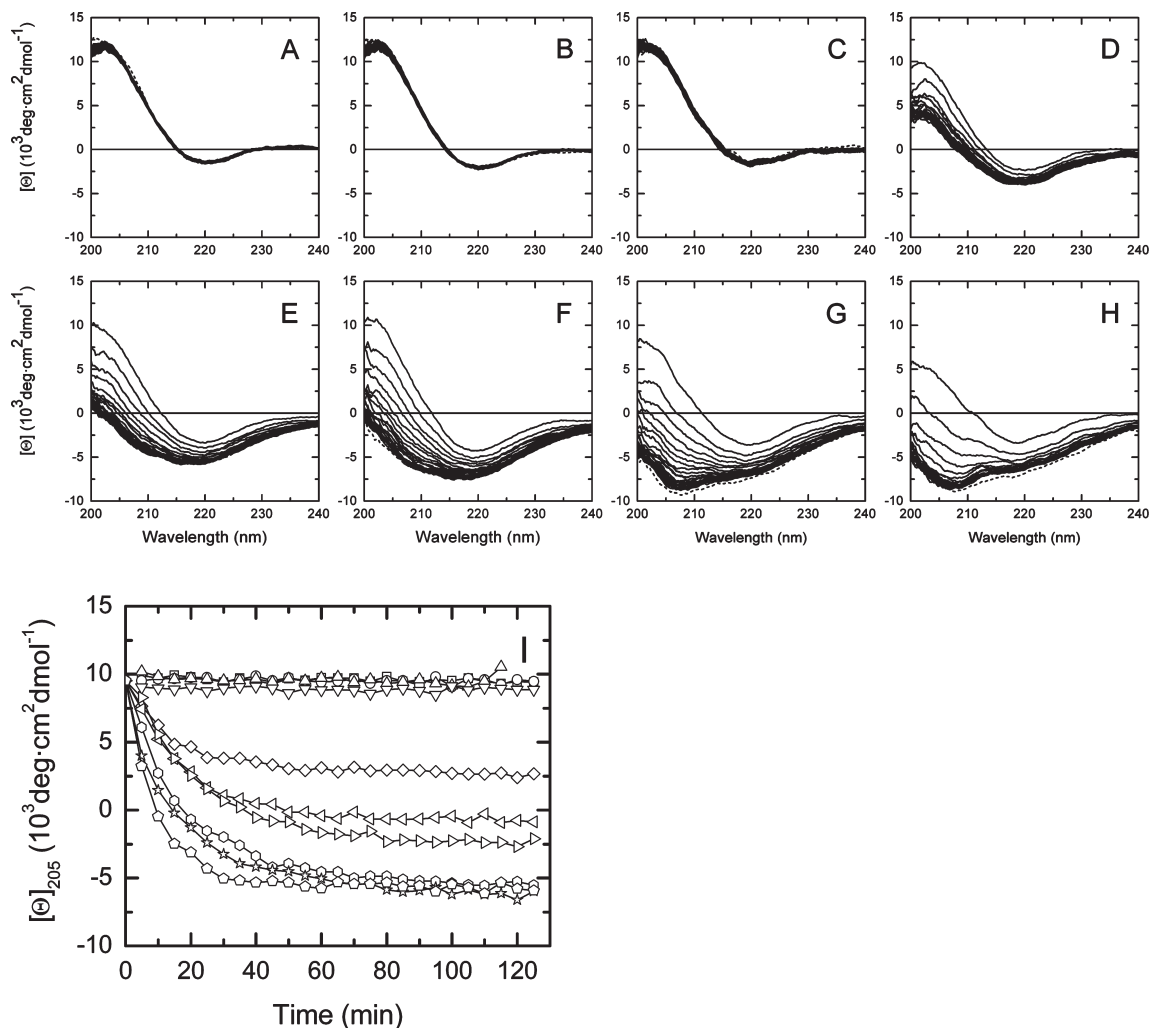


FIGURE 4: Effect of different LPA concentrations on the secondary structure of native  $\beta 2\text{m}$ .  $\beta 2\text{m}$  monomers were incubated at  $37^\circ\text{C}$  for 2 h in the absence of any additives (A), in the presence of  $500 \mu\text{M}$  LPC (B), and in the presence of  $150 \mu\text{M}$  (C),  $200 \mu\text{M}$  (D),  $300 \mu\text{M}$  (E),  $400 \mu\text{M}$  (F),  $500 \mu\text{M}$  (G), and  $700 \mu\text{M}$  (H) LPA. Far-UV CD spectra were recorded at every 5 min. Reaction mixtures contained  $0.1 \text{ mg/mL}$  monomeric  $\beta 2\text{m}$  in  $50 \text{ mM}$  sodium phosphate and  $100 \text{ mM}$  NaCl, pH 7.5. Dotted lines represent spectra at an incubation time of 24 h. Note that spectra obtained at 2 and 24 h are overlapping. (I) Kinetics of the mean residue ellipticity ( $[\theta]$ ) at  $205 \text{ nm}$  as a function of LPA concentration: ( $\square$ )  $0 \mu\text{M}$ , ( $\circ$ )  $100 \mu\text{M}$ , ( $\nabla$ )  $150 \mu\text{M}$ , ( $\diamond$ )  $200 \mu\text{M}$ , ( $\triangleleft$ )  $300 \mu\text{M}$ , ( $\triangleright$ )  $400 \mu\text{M}$ , ( $\odot$ )  $500 \mu\text{M}$ , ( $\star$ )  $600 \mu\text{M}$ , ( $\oplus$ )  $700 \mu\text{M}$  LPA, and ( $\Delta$ )  $500 \mu\text{M}$  LPC.

leads to destabilization of the native structure. Limited proteolysis can be used as a sensitive probe for protein unfolding (43). Chymotrypsin was chosen because native  $\beta 2\text{m}$  is relatively resistant against chymotryptic degradation. Chymotrypsin cleaves at the carboxyl sides of aromatic or bulky nonpolar side chains, which are mostly buried in the native structure. The phosphate moiety in sodium phosphate buffer might compete with the phosphate headgroup of LPA, which would result in an apparent elevation of the threshold for protein destabilization; therefore, we conducted these experiments in HEPES buffer, as well.

Our results indicate that LPA destabilizes the native  $\beta 2\text{m}$  as proteolytic products appear in the presence of LPA (Figure 6). In  $50 \text{ mM}$  HEPES buffer, cleavage products appeared at  $25 \mu\text{M}$  and higher LPA, while they were unambiguously observable from  $50 \mu\text{M}$  LPA in  $50 \text{ mM}$  sodium phosphate buffer. LPC did not affect the proteolytic cleavability of  $\beta 2\text{m}$  (see Supporting Information Figure 1).

**Effect of Monomer Conformation on the Polymerization Reaction.** The destabilizing effect of LPA on the structure of native  $\beta 2\text{m}$  monomers takes place in a time scale of 1 h as presented above. To study whether the native molecule or the

partially unfolded species elongate the preformed seeds, additional polymerization experiments were carried out (Figure 7). In one set of samples,  $\beta 2\text{m}$  monomers were preincubated at  $37^\circ\text{C}$  for 70 min with  $300 \mu\text{M}$  LPA before inducing the fibril formation by seeds. In the other set of samples, the monomeric protein and seeds were added to the lipid solution simultaneously. Seeds grown at pH 7.5 were used for both cases, and fibril growth was monitored by the increase of ThT fluorescence. Without preincubation, a significantly lower growth rate was observed for about 20 min, compared to the preincubated sample (Figure 7). This indicates that a partially unfolded intermediate is required for fibril extension.

**Effect of LPA on the Stability of Monomeric  $\beta 2\text{m}$  Revealed by DSC.** To investigate the effect of LPA on the structural stability of native monomeric  $\beta 2\text{m}$ , DSC measurements were carried out at different LPA concentrations (Figure 8). Without additives,  $\beta 2\text{m}$  exhibits a cooperative unfolding transition with a melting temperature of  $64.6^\circ\text{C}$ . The addition of either  $50 \mu\text{M}$  LPA or  $500 \mu\text{M}$  LPC has no significant effect on the thermal unfolding of the protein. In the presence of 100 and  $200 \mu\text{M}$  LPA, the height of the unfolding peaks decreases significantly, entailing the loss of more than 75% of the peak

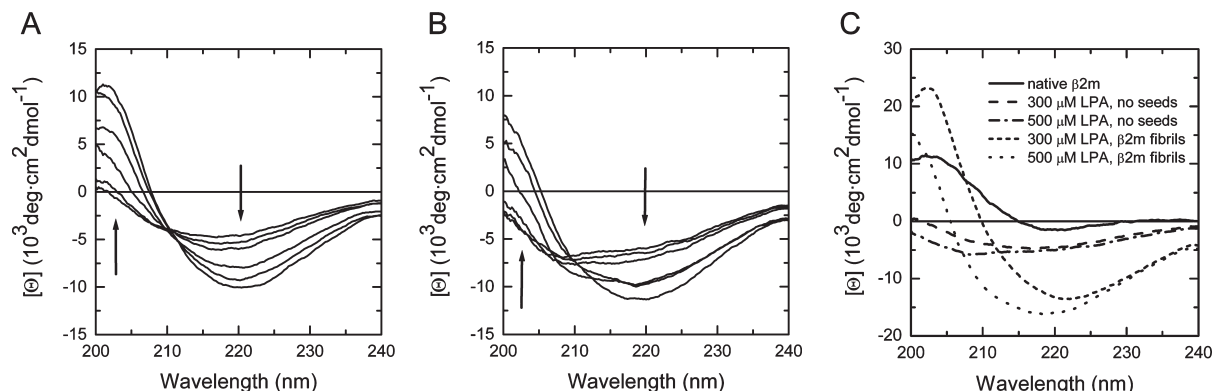


FIGURE 5: Far-UV CD spectra of  $\beta 2m$  amyloid fibrils formed in the presence of LPA and pH 7.5 seeds. CD spectra were recorded after 0, 1, 4, 20, 30, and 48 h of incubation at 37 °C in the presence of 300  $\mu M$  (A) and 500  $\mu M$  (B) LPA. The reaction mixture contained 0.1 mg/mL monomeric  $\beta 2m$  in 50 mM sodium phosphate and 100 mM NaCl, pH 7.5. Seed concentration was 10  $\mu g/mL$ . Before the seed-induced fibril formation,  $\beta 2m$  monomers were preincubated for 2 h in the presence of the lipid. Arrows show the direction of changes. (C) Comparison of the secondary structure of different conformations of  $\beta 2m$ . The figure shows the mean residue ellipticity of native  $\beta 2m$  (—),  $\beta 2m$  incubated for 24 h in the presence of 300  $\mu M$  (—) and 500  $\mu M$  (— · —) LPA with no seeds, and  $\beta 2m$  samples inoculated with 10  $\mu g/mL$  seeds prepared from fifth generation fibrils and incubated for 1 week in the presence 300  $\mu M$  (---) and 500  $\mu M$  (· · ·) LPA.

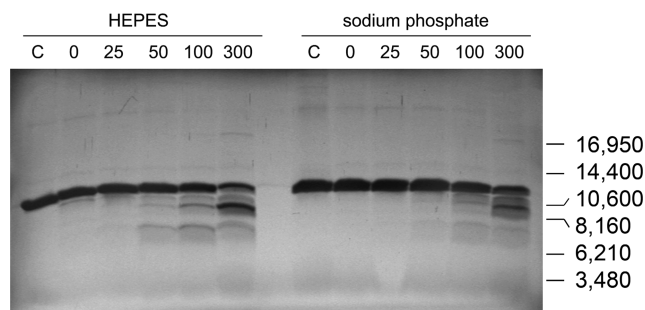


FIGURE 6: Limited proteolysis of monomeric  $\beta 2m$  by chymotrypsin as a function of LPA concentration.  $\beta 2m$  (0.2 mg/mL) was preincubated in either 50 mM HEPES or 50 mM sodium phosphate, pH 7.5, containing 100 mM NaCl and different concentrations of LPA, as indicated in the figure, at 37 °C for 1 h. Chymotryptic proteolysis was conducted for 30 min; the enzyme: $\beta 2m$  molar ratio was 1:100. Proteolysis was analyzed by running the samples in 16.5% Tris/Tricine SDS–polyacrylamide gels. Lanes “C” show undigested controls.

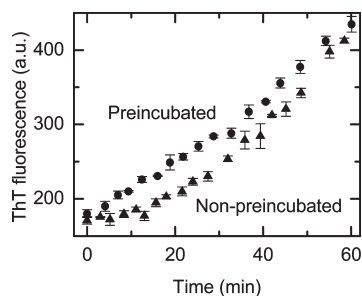


FIGURE 7: Seeded polymerization reaction of  $\beta 2m$  with and without preincubation of the monomers with LPA. (●)  $\beta 2m$  monomers were preincubated at 37 °C for 70 min in the presence of 300  $\mu M$  LPA before inducing fibril formation by the addition of seeds. (▲) Slower initial fibril growth was observed when LPA and seeds were added to the  $\beta 2m$  solution simultaneously. Samples contained 0.1 mg/mL monomer  $\beta 2m$  in 50 mM sodium phosphate and 100 mM NaCl, pH 7.5. Ten  $\mu g/mL$  seeds grown at pH 7.5 were used. Fibril growth was monitored by ThT fluorescence. Data points are mean  $\pm$  standard error of three independent measurements.

area at 200  $\mu M$  LPA. A decrease in the peak area, i.e., in calorimetric enthalpy, without significant change in the melting temperature suggests that the number of native molecules

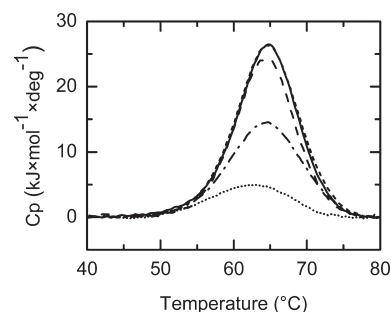


FIGURE 8: Calorimetric melting profile of  $\beta 2m$  in the presence of LPA and LPC. Samples containing 0.1 mg/mL  $\beta 2m$  and 0  $\mu M$  (—), 50  $\mu M$  (---), 100  $\mu M$  (— · —), 200  $\mu M$  (· · ·) LPA, and 500  $\mu M$  LPC (— —) in 50 mM sodium phosphate and 100 mM NaCl, pH 7.5, were heated at a rate of 1 °C/min.

decreases with increasing LPA concentration. Because no other cooperative unfolding peaks appeared in the heating profile, a plausible interpretation is that LPA destabilizes the structure of  $\beta 2m$  and the LPA-bound protein exhibits no cooperative unfolding transition. A slight decrease (about 2 °C) in the melting temperature was observed at 200  $\mu M$  LPA concentration, further indicating that LPA destabilizes the protein's native structure.

**ANS Binding of Monomeric  $\beta 2m$ .** As presented in detail in Supporting Information Figure 3, LPA-destabilized  $\beta 2m$  exhibited enhanced ANS fluorescence. The time course of the fluorescence increase is in good agreement with the CD spectroscopy results regarding the kinetics of the structural changes. Native  $\beta 2m$  showed no ANS fluorescence. Enhancement of ANS fluorescence is one hallmark of the molten globule-like state of proteins.

**Effect of LPA on the Stability of  $\beta 2m$  Fibrils.** In another work, we found that amyloid fibrils dissociate at elevated temperatures, and SDS protects them from thermal-induced depolymerization.<sup>2</sup> Here, we examined the stabilization effect of LPA on the fibrils against heat treatment at pH 2.5. Under this nonphysiological condition, fibrils could be produced in the absence of additives (4–8), making it possible to study the effect of each lipid separately. Moreover, monomeric  $\beta 2m$  is disordered

<sup>2</sup>J. Kardos, A. Micsonai, E. Petrik, H. Naiki, L. Gráf, and Y. Goto, unpublished results.



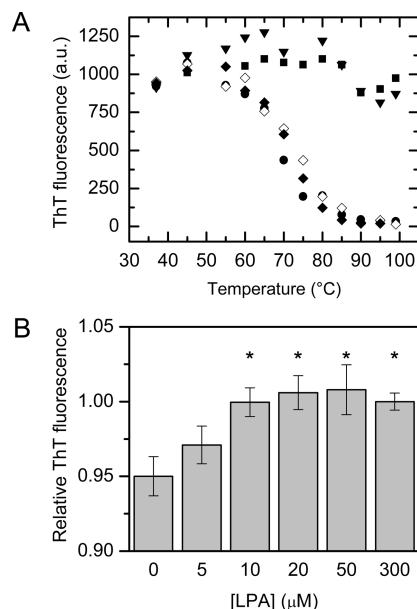


FIGURE 9: Effect of LPA on the stability of amyloid fibrils. (A) Effect of LPA and related analogues on the thermal stability of  $\beta$ 2m fibrils. Amyloid fibrils grown at pH 2.5 were heat-treated at different temperatures for 5 min in the presence of SDS (▼), LPA (■), LPC (●), and SPC (◆). The remaining fibril content was monitored by ThT fluorescence. The initial fibril concentration was 0.1 mg/mL. The reaction mixture contained 50 mM sodium citrate, 100 mM NaCl, pH 2.5, and 500  $\mu$ M different additives. LPA and SDS stabilized the fibrils preventing them from dissociation, while the other lipids exhibited no effect on fibril stability compared to the lipid-free control (◇). A typical experiment of three determinations is shown. The experimental error was less than 10%. (B) Depolymerization of fibrils in the presence of LPA. Amyloid fibrils, grown at pH 7.5, at a concentration of 0.05 mg/mL, were incubated at 37 °C for 2 months in the presence of different concentrations of LPA as indicated below the columns. The remaining fibril content was monitored by ThT fluorescence. LPA completely prevented the depolymerization of fibrils at a concentration as low as 10  $\mu$ M. Columns represent mean  $\pm$  standard error of five independent measurements. Asterisks mark significant differences as compared to the control (no LPA) experiment as revealed by Student's *t* test ( $p < 0.05$ ).

at this low pH, giving the opportunity to selectively study fibril stability. Preformed fibrils were incubated at various temperatures for 5 min, and the remaining ThT fluorescence was measured (Figure 9A). It was found that 500  $\mu$ M LPA prevented fibrils from heat-induced dissociation, while the other lipids (LPC and SPC) had no effect.

We also studied the effect of LPA on the stability of fibrils under physiological conditions following the depolymerization of tenth generation fibrils, formed at pH 7.5 and 300  $\mu$ M LPA. After removal of LPA by repeated washing, these fibrils exhibited surprising stability, showing only slow depolymerization. Thus we monitored the remaining fibril content for a prolonged period of time. The fibrils were resuspended in a lipid-free buffer or in the presence of 5–300  $\mu$ M LPA and incubated at 37 °C. The stabilizing effect of LPA was elucidated after 2 months of incubation (Figure 9B). As can be seen, LPA completely prevented  $\beta$ 2m fibrils from depolymerization even at a concentration as low as 10  $\mu$ M, well below CMC.

**Interaction of  $\beta$ 2m with LPA Micelles Studied by ITC.** Similarly to SDS, lysophospholipids in water-based buffer solutions form micelles in a concentration-dependent manner. To better understand the interaction of LPA with  $\beta$ 2m, it is essential to examine whether the observed effect is caused by LPA

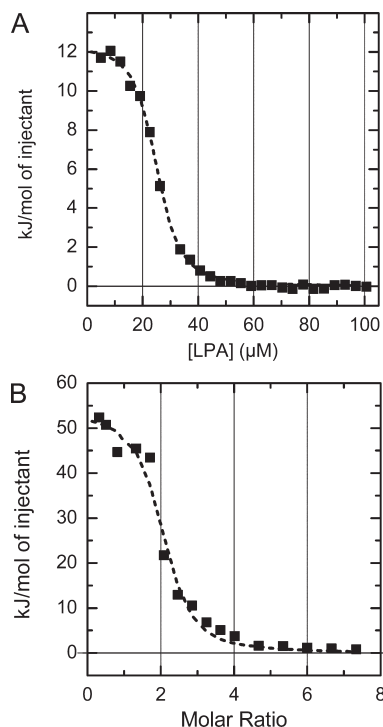


FIGURE 10: Micelle formation of LPA and micelle- $\beta$ 2m interaction investigated by ITC. (A) Determination of critical micelle concentration of LPA. Enthalpy changes corresponding to the dissociation of micelles were followed by repeated injections of 1 mM LPA into the calorimeter cell at 37 °C. A buffer solution containing 50 mM sodium phosphate and 100 mM NaCl, pH 7.5, was used in both the cell and injection syringe. (B) LPA micelle- $\beta$ 2m interaction was measured by injecting 470  $\mu$ M  $\beta$ 2m into the cell containing 300  $\mu$ M LPA. The line shows a fitted saturation curve assuming the binding of two  $\beta$ 2m molecules to one LPA micelle, yielding a dissociation constant of  $520 \pm 200$  nM.

monomers or the micellar form. Critical micelle concentrations (CMC) of LPA and LPC were determined under the same conditions applied in our other experiments. A solution containing 1 mM LPA, which is expected to exceed CMC, was successively injected into the calorimeter cell that contained only buffer at the beginning. At concentrations fairly below CMC, the injected lipid micelles dissociated via an endothermic reaction taking up significant heat. With LPA concentrations increasing above CMC in the cell, the injected micelles remained intact, exhibiting no further heat effect. The results indicated a CMC value of approximately 50  $\mu$ M for LPA (Figure 10A). Using another definition for CMC introduced by Li et al. (34), i.e., the concentration belonging to the inflection point of the ITC profile, the CMC value was approximated as 25  $\mu$ M. The CMC value of LPC, measured by the injection of 500  $\mu$ M LPC into the ITC cell, was proven to be 5–10  $\mu$ M (data not shown). The 25–700  $\mu$ M concentration range of LPA, that was shown to be effective on monomeric  $\beta$ 2m in the present work, falls into the micelle-forming region. This suggests that the nature of the interaction between LPA and monomeric  $\beta$ 2m is a lipid micelle-protein interaction.

To further characterize the interaction of  $\beta$ 2m with LPA micelles, titration experiments were carried out by injecting monomeric  $\beta$ 2m into the ITC cell containing 300  $\mu$ M LPA (Figure 10B). To estimate the concentration of micelles in the ITC cell, we assumed that a micelle consists of approximately 60 LPA molecules, based on the work of Tanford (44) and the fact that micelles have a narrow size distribution. Figure 10B shows



the titration with an acceptable saturation curve fit using an estimated micelle concentration of 5  $\mu\text{M}$ . Surprisingly, the titration curve indicates that LPA micelles can be saturated by  $\beta 2\text{m}$  molecules with a 1:2 stoichiometric ratio. The positively charged side chains of  $\beta 2\text{m}$  are enriched on one side of the molecule (see Protein Data Bank entry 2yxf, published in ref (45)). It is a reasonable assumption that the negatively charged surface of one LPA micelle can be surrounded by two  $\beta 2\text{m}$  molecules facing with their positive sides to the micelle. The  $520 \pm 200$  nM dissociation equilibrium constant indicates high-affinity binding of monomeric  $\beta 2\text{m}$  to LPA micelles. The reaction is entropy driven with an endothermic enthalpy change of  $54 \pm 3$  kJ/mol. This value is comparable to the 175 kJ/mol unfolding  $\Delta H$  of native  $\beta 2\text{m}$  at 37 °C (46), suggesting a considerable disruption of the interactions that stabilize the native structure of  $\beta 2\text{m}$ .

## DISCUSSION

An elevated concentration of  $\beta 2\text{m}$ , observed in DRA, is insufficient for amyloid formation *in vitro* at neutral pH (9). Various molecules were identified which might contribute to the amyloid formation of  $\beta 2\text{m}$  at neutral pH, as presented in the introduction. These molecules can, on one hand, destabilize the structure of monomeric  $\beta 2\text{m}$  which seems to be essential for amyloid formation (9, 47–52). On the other hand, they can stabilize the preformed fibrils and prevent them from depolymerization (11–14, 22). However, the detailed mechanism of fibril formation still remained elusive.

The role of lipid–protein interactions in amyloid fibril formation has been reviewed by Gorbenko and Kinnunen (53); however, they primarily focused on the role of membrane lipids. Gellermann et al. in a comparative study determined the chemical composition of the lipid components from disease-associated amyloid deposits including  $\beta 2\text{m}$  fibrils (54). They found that these amyloid deposits contain significant amounts of lipids, an average of 7% in the case of  $\beta 2\text{m}$  deposits. Hagihara et al. showed that anionic lysophospholipids induce aggregation of  $\beta 2$ -glycoprotein (55). Ookoshi et al. (24) screened for lysophospholipids that have an effect on amyloid formation of  $\beta 2\text{m}$ . Varying the headgroup and the length and saturation of the hydrophobic tail, they found lysophosphatidic acids to be the most effective. In the present work, we investigated the mechanism of LPA action on the process of  $\beta 2\text{m}$  amyloid formation. For comparison, we included LPC, the precursor lipid of LPA abundant in blood, as well as the structurally and physiologically related blood-born sphingolipid mediators SIP and SPC.

**LPA Induces Amyloid Formation of  $\beta 2\text{m}$  at Neutral pH.** We carried out experiments under physiological conditions concerning pH, ionic strength, and temperature, as well as  $\beta 2\text{m}$  concentration in patients with end-stage DRA (56, 57). We demonstrated that LPA induces amyloid fibril formation at neutral pH in a nucleation-dependent manner as revealed by ThT fluorescence measurements, CD spectroscopy, and electron microscopy (Figures 1, 3, and 5). On the contrary, the other lipids had no effect on amyloid fibril formation.

LPA-induced fibril extension was significantly faster using seeds prepared from fibrils grown at neutral pH in the presence of LPA compared to seeds prepared from low-pH fibrils (Figures 1 and 2). Additionally, the final ThT intensity reached the end value measured in polymerization at low pH. This indicates a complete polymerization where nearly all  $\beta 2\text{m}$  molecules are converted into amyloid fibrils, similarly to the reaction at pH 2.5,

where a remaining monomer concentration around 1% of the initial value was observed (46). We observed another important difference between fibrils grown at neutral pH in the presence of LPA compared to the low-pH fibrils. Using seeds preformed at pH 2.5, fibril formation at pH 7.5 showed an initial depolymerization. This was not observable when seeds formed at pH 7.5 were used; furthermore, these fibrils depolymerize unexpectedly slowly after the removal of LPA. These findings indicate that the molecular organization of fibrils formed under physiological conditions differs from that of fibrils formed at pH 2.5.

Studying the effect of lysophospholipids on the amyloid formation of  $\beta 2\text{m}$ , Ookoshi et al. (24) used seeds prepared from fibrils grown in the presence of SDS. They observed less than 50% of the ThT fluorescence intensity compared to that of SDS-induced growth, indicating that only a part of  $\beta 2\text{m}$  monomers were incorporated into fibrils. The fact that seeds grown in the presence of LPA can induce complete polymerization suggests that SDS and LPA have different effects on amyloid formation.

**The Amyloidogenic Intermediate Is a Partially Unfolded Molecule.** In the absence of amyloid seeds fibril formation was not initiated by LPA during the time course of our experiments (up to 1 week). However, LPA destabilizes the structure of native monomeric  $\beta 2\text{m}$  as revealed by far-UV CD spectra (Figure 4), limited proteolysis (Figure 6), and DSC (Figure 8). Cross-linking studies have proved that LPA-destabilized  $\beta 2\text{m}$  remains monomeric; it does not form dimers in detectable amount (Supporting Information Figure 2). Additionally, the LPA-bound form exhibited no cooperative unfolding transition in DSC experiments and showed increased ANS fluorescence (Supporting Information Figure 3), similarly to a partially unfolded state such as a molten globule. Structural changes elicited by LPA reached an equilibrium within 1–2 h (Figure 4I). Accordingly, fibril formation was instant when polymerization was initiated after about 1 h preincubation of  $\beta 2\text{m}$  monomers with LPA. On the contrary, when seeds and LPA were added simultaneously, a lower growth rate was observed in the first 20–30 min (Figure 7). These results prove that native  $\beta 2\text{m}$  is not capable of extending the seeds; rather, partially unfolded forms have amyloidogenic properties.

Amyloid fibril formation was most efficient around 300  $\mu\text{M}$  LPA (Figure 2). The presence of an isodichroic point in the CD spectra at this concentration (Figure 5A) implicates that two conformational species of  $\beta 2\text{m}$  dominate in the solution, i.e., amyloid fibrils and partially unfolded monomers. At 500  $\mu\text{M}$  LPA, no isodichroic point can be observed, indicating the presence of more than two conformational states (Figure 5B). Secondary structure estimation from CD spectra of monomeric  $\beta 2\text{m}$  (Supporting Information Table 1) shows a decrease in the  $\beta$ -sheet content at 300  $\mu\text{M}$  LPA. Above this LPA concentration, the structure of monomers becomes more unfolded, whose form is less favorable for fibril extension.

In conclusion, the amyloidogenic intermediate of  $\beta 2\text{m}$  is a moderately unfolded species that is most populated around 300  $\mu\text{M}$  LPA concentration. These observations are consistent with previous studies reporting that amyloid formation proceeds via partially unfolded intermediates (9, 47–52). We can find a notable similarity between TFE, SDS, and LPA in the context that they are most effective at moderately denaturing concentrations where the tertiary structure of native  $\beta 2\text{m}$  is destabilized, resulting in a partially unfolded state of the molecule (12, 22, 58). However, TFE exhibits its effect at significantly higher concentrations as a cosolvent, by altering the solvent properties and

modulating the balance of hydrogen bonds and hydrophobic interactions.

We suppose that LPA can bind  $\beta 2m$  through electrostatic interactions. In this respect it is similar to collagen, but in that case the positively charged residues on the collagen fibril surface might be involved in the interaction with  $\beta 2m$  (17, 18). In contrast, the headgroup of LPA is negatively charged and may interact primarily with lysine and arginine residues of  $\beta 2m$ . Copper ions also induce fibril formation under physiological conditions. Copper binding is localized to His31 and Trp60 of native  $\beta 2m$ . Unlike LPA, copper does not cause significant changes in the CD spectrum of the native protein; however, it destabilizes  $\beta 2m$  against thermal and urea denaturation (19–21) and catalyzes oligomerization (48, 59).

**LPA Stabilizes the Amyloid Fibrils.** Below 100  $\mu M$  LPA the stable native conformation of  $\beta 2m$  is predominant as revealed by CD spectroscopy (Figure 4), and only a low level of the partially unfolded form is present according to limited proteolysis (Figure 6). The fact that amyloid fibril growth proved to be significant at this concentration (Figure 2) suggests that LPA exhibits a stabilizing effect on the amyloid fibrils.

Based on the observation that, at pH 2.5,  $\beta 2m$  fibrils dissociate at high temperature,<sup>2</sup> the effect of LPA on fibril stability was first probed by incubating preformed fibrils at elevated temperatures. These experiments revealed that LPA, similarly to SDS, stabilizes fibrils, preventing them from dissociation. In contrast, the other investigated lipids exhibited no detectable effect (Figure 9A).

Furthermore, we observed that  $\beta 2m$  fibrils, grown at pH 7.5, exhibited surprising resistance against depolymerization after removal of LPA (Figure 9B) at 37 °C. Nevertheless, the slow dissociation in the absence of LPA could be completely blocked by the presence of only 10  $\mu M$  LPA (Figure 9B). These results also depict the difference between  $\beta 2m$  fibrils grown at low and physiological pH, the existence of which has been an open question (8, 60). Our observations emphasize the importance to study the amyloid formation of  $\beta 2m$  at physiological pH.

**$\beta 2m$  Interacts with an Aggregated Form of LPA.** At an LPA concentration of approximately 25–50  $\mu M$  and above, the micellar form of the lipid is present *in vitro* (Figure 10). Fibril formation induced by LPA was observed above the CMC, showing that  $\beta 2m$  monomers interact with LPA micelles *in vitro*. Based on the estimate of an average of 60 lipids per micelle, the concentration of micelles is in the range of low micromoles. By ITC measurements, we identified a high-affinity interaction between LPA micelles and  $\beta 2m$  *in vitro* ( $K_D = 520 \pm 200$  nM). In contrast to LPA, the effective concentration range of SDS to induce  $\beta 2m$  amyloid fibril formation is below its CMC (22, 23), further emphasizing a difference in the mechanism of action of LPA and SDS.

**Physiological Relevance of the Amyloidogenic Effect of LPA.** LPA is present in biological fluids, raising a possible *in vivo* relevance of our findings for DRA. According to a recent study, the average serum concentration of LPA in healthy individuals is about 3  $\mu M$  (61). On the contrary, in some ovarian cancer patients concentrations as high as 15–20  $\mu M$  were detected (61). Presumably, these values can be manifold higher locally at the site of production, reaching the effective concentration range in this work. About a 3-fold elevation of plasma LPA (from 0.5 to 1.4  $\mu M$ , taken before dialysis) was reported in patients undergoing long-term hemodialysis compared to healthy controls (24, 62). It is well-known that the contact with dialysis membrane activates several blood cells including platelets (63, 64). The activated

platelets produce LPA (65), which should further increase its concentration. Future studies are needed to measure the peak LPA concentrations in patients following the dialysis procedures. Gellermann et al. observed the presence of LPC, the precursor of LPA, in  $\beta 2m$  amyloid deposits in patients, though LPA was not measured (54). They proposed that the lipid enrichment represents an additional factor affecting the clinical deposition of amyloid.

In our experiments, the polymerization of  $\beta 2m$  is completed in hours or days, while the development of DRA is a slow process taking several years. This might be the consequence of the *in vivo* average lower level of LPA compared to our *in vitro* model system. The temporary and local bursts in the concentration of  $\beta 2m$ -destabilizing agents such as LPA and the low depolymerization rate of the fibrils formed at physiological conditions together with the potent stabilizing effect of LPA on the amyloid fibrils might give an explanation for the development of DRA.

In summary, LPA induces amyloid formation through a dual mechanism. It is an amyloidogenic factor that destabilizes the structure of monomeric  $\beta 2m$ , inducing a partially unfolded intermediate state. This form is capable of fibril extension in the presence of preformed fibril seeds. On the other hand, LPA stabilizes the  $\beta 2m$  amyloid fibrils. Although many factors can interplay in the development of DRA, we propose that LPA might be one among the physiologically relevant molecules exhibiting synergistic effect on fibril formation.

## SUPPORTING INFORMATION AVAILABLE

We estimated the secondary structure content of the different forms of monomeric  $\beta 2m$  from their CD spectra using various methods. The results are presented in Supplementary Table 1. Although different prediction algorithms provided different values, we could observe clear tendencies in the secondary structure changes. LPC did not affect the proteolytic cleavability of  $\beta 2m$ , which was verified by SDS–PAGE and shown in Supplementary Figure 1. Cross-linking studies have proved that LPA-destabilized  $\beta 2m$  is monomeric. The results are presented in Supplementary Figure 2. Monomeric  $\beta 2m$  in the presence of LPA showed increased ANS fluorescence indicating the formation of a molten globule-like intermediate (Supplementary Figure 3). This material is available free of charge via the Internet at <http://pubs.acs.org>.

## REFERENCES

1. Rochet, J. C., and Lansbury, P. T. Jr. (2000) Amyloid fibrillogenesis: themes and variations. *Curr. Opin. Struct. Biol.* 10, 60–68.
2. Stefani, M., and Dobson, C. M. (2003) Protein aggregation and aggregate toxicity: new insights into protein folding, misfolding diseases and biological evolution. *J. Mol. Med.* 81, 678–699.
3. Gejyo, F., Yamada, T., Odani, S., Nakagawa, Y., Arakawa, M., Kunitomo, T., Kataoka, H., Suzuki, M., Hirasawa, Y., and Shirahama, T.; et al. (1985) A new form of amyloid protein associated with chronic hemodialysis was identified as beta 2-microglobulin. *Biochem. Biophys. Res. Commun.* 129, 701–706.
4. Naiki, H., Hashimoto, N., Suzuki, S., Kimura, H., Nakakuki, K., and Gejyo, F. (1997) Establishment of a kinetic model of dialysis-related amyloid fibril extension *in vitro*. *Amyloid* 4, 223–232.
5. Kad, N. M., Thomson, N. H., Smith, D. P., Smith, D. A., and Radford, S. E. (2001) Beta(2)-microglobulin and its deamidated variant, N17D form amyloid fibrils with a range of morphologies *in vitro*. *J. Mol. Biol.* 313, 559–571.
6. Ban, T., Hamada, D., Hasegawa, K., Naiki, H., and Goto, Y. (2003) Direct observation of amyloid fibril growth monitored by thioflavin T fluorescence. *J. Biol. Chem.* 278, 16462–16465.

7. Ohhashi, Y., Kihara, M., Naiki, H., and Goto, Y. (2005) Ultrasonication-induced amyloid fibril formation of beta2-microglobulin. *J. Biol. Chem.* 280, 32843–32848.
8. Kardos, J., Okuno, D., Kawai, T., Hagihara, Y., Yumoto, N., Kitagawa, T., Zavodszky, P., Naiki, H., and Goto, Y. (2005) Structural studies reveal that the diverse morphology of beta(2)-microglobulin aggregates is a reflection of different molecular architectures. *Biochim. Biophys. Acta* 1753, 108–120.
9. McParland, V. J., Kad, N. M., Kalverda, A. P., Brown, A., Kirwin-Jones, P., Hunter, M. G., Sunde, M., and Radford, S. E. (2000) Partially unfolded states of beta(2)-microglobulin and amyloid formation in vitro. *Biochemistry* 39, 8735–8746.
10. Ohashi, K., Kisilevsky, R., and Yanagishita, M. (2002) Affinity binding of glycosaminoglycans with beta(2)-microglobulin. *Nephron* 90, 158–168.
11. Yamaguchi, I., Suda, H., Tsuzuki, N., Seto, K., Seki, M., Yamaguchi, Y., Hasegawa, K., Takahashi, N., Yamamoto, S., Gejyo, F., and Naiki, H. (2003) Glycosaminoglycan and proteoglycan inhibit the depolymerization of beta2-microglobulin amyloid fibrils in vitro. *Kidney Int.* 64, 1080–1088.
12. Yamamoto, S., Yamaguchi, I., Hasegawa, K., Tsutsumi, S., Goto, Y., Gejyo, F., and Naiki, H. (2004) Glycosaminoglycans enhance the trifluoroethanol-induced extension of beta2-microglobulin-related amyloid fibrils at a neutral pH. *J. Am. Soc. Nephrol.* 15, 126–133.
13. Myers, S. L., Jones, S., Jahn, T. R., Morten, I. J., Tennent, G. A., Hewitt, E. W., and Radford, S. E. (2006) A systematic study of the effect of physiological factors on beta2-microglobulin amyloid formation at neutral pH. *Biochemistry* 45, 2311–2321.
14. Yamaguchi, I., Hasegawa, K., Takahashi, N., Gejyo, F., and Naiki, H. (2001) Apolipoprotein E inhibits the depolymerization of beta 2-microglobulin-related amyloid fibrils at a neutral pH. *Biochemistry* 40, 8499–8507.
15. Ono, K., and Uchino, F. (1994) Formation of amyloid-like substance from beta-2-microglobulin in vitro. Role of serum amyloid P component: a preliminary study. *Nephron* 66, 404–407.
16. Homma, N., Gejyo, F., Isemura, M., and Arakawa, M. (1989) Collagen-binding affinity of beta-2-microglobulin, a preprotein of hemodialysis-associated amyloidosis. *Nephron* 53, 37–40.
17. Giorgetti, S., Rossi, A., Mangione, P., Raimondi, S., Marini, S., Stoppini, M., Corazza, A., Viglino, P., Esposito, G., Cetta, G., Merlini, G., and Bellotti, V. (2005) Beta2-microglobulin isoforms display an heterogeneous affinity for type I collagen. *Protein Sci.* 14, 696–702.
18. Relini, A., Canale, C., De Stefano, S., Rolandi, R., Giorgetti, S., Stoppini, M., Rossi, A., Fogolari, F., Corazza, A., Esposito, G., Giozzi, A., and Bellotti, V. (2006) Collagen plays an active role in the aggregation of beta2-microglobulin under physiopathological conditions of dialysis-related amyloidosis. *J. Biol. Chem.* 281, 16521–16529.
19. Morgan, C. J., Gelfand, M., Atreya, C., and Miranker, A. D. (2001) Kidney dialysis-associated amyloidosis: a molecular role for copper in fiber formation. *J. Mol. Biol.* 309, 339–345.
20. Eakin, C. M., Knight, J. D., Morgan, C. J., Gelfand, M. A., and Miranker, A. D. (2002) Formation of a copper specific binding site in non-native states of beta-2-microglobulin. *Biochemistry* 41, 10646–10656.
21. Villanueva, J., Hoshino, M., Katou, H., Kardos, J., Hasegawa, K., Naiki, H., and Goto, Y. (2004) Increase in the conformational flexibility of beta 2-microglobulin upon copper binding: a possible role for copper in dialysis-related amyloidosis. *Protein Sci.* 13, 797–809.
22. Yamamoto, S., Hasegawa, K., Yamaguchi, I., Tsutsumi, S., Kardos, J., Goto, Y., Gejyo, F., and Naiki, H. (2004) Low concentrations of sodium dodecyl sulfate induce the extension of beta2-microglobulin-related amyloid fibrils at a neutral pH. *Biochemistry* 43, 11075–11082.
23. Kihara, M., Chatani, E., Sakai, M., Hasegawa, K., Naiki, H., and Goto, Y. (2005) Seeding-dependent maturation of beta2-microglobulin amyloid fibrils at neutral pH. *J. Biol. Chem.* 280, 12012–12018.
24. Ookoshi, T., Hasegawa, K., Ohhashi, Y., Kimura, H., Takahashi, N., Yoshida, H., Miyazaki, R., Goto, Y., and Naiki, H. (2008) Lysophospholipids induce the nucleation and extension of {beta}2-microglobulin-related amyloid fibrils at a neutral pH. *Nephrol. Dial. Transplant.* 23, 3247–3255.
25. Tigyi, G., and Miledi, R. (1992) Lysophosphatidates bound to serum albumin activate membrane currents in *Xenopus* oocytes and neurite retraction in PC12 pheochromocytoma cells. *J. Biol. Chem.* 267, 21360–21367.
26. Moolenaar, W. H., van Meeteren, L. A., and Giepmans, B. N. (2004) The ins and outs of lysophosphatidic acid signaling. *BioEssays* 26, 870–881.
27. Tokumura, A. (2002) Physiological and pathophysiological roles of lysophosphatidic acids produced by secretory lysophospholipase D in body fluids. *Biochim. Biophys. Acta* 1582, 18–25.
28. Tigyi, G., and Parrill, A. L. (2003) Molecular mechanisms of lysophosphatidic acid action. *Prog. Lipid Res.* 42, 498–526.
29. Chiba, T., Hagihara, Y., Higurashi, T., Hasegawa, K., Naiki, H., and Goto, Y. (2003) Amyloid fibril formation in the context of full-length protein: effects of proline mutations on the amyloid fibril formation of beta2-microglobulin. *J. Biol. Chem.* 278, 47016–47024.
30. Naiki, H., and Gejyo, F. (1999) Kinetic analysis of amyloid fibril formation. *Methods Enzymol.* 309, 305–318.
31. Deleage, G., and Geourjon, C. (1993) An interactive graphic program for calculating the secondary structure content of proteins from circular dichroism spectrum. *Comput. Appl. Biosci.* 9, 197–199.
32. Schagger, H., and von Jagow, G. (1987) Tricine-sodium dodecyl sulfate-polyacrylamide gel electrophoresis for the separation of proteins in the range from 1 to 100 kDa. *Anal. Biochem.* 166, 368–379.
33. Lesse, A. J., Campagnari, A. A., Bittner, W. E., and Apicella, M. A. (1990) Increased resolution of lipopolysaccharides and lipooligosaccharides utilizing tricine-sodium dodecyl sulfate-polyacrylamide gel electrophoresis. *J. Immunol. Methods* 126, 109–117.
34. Li, Z., Mintzer, E., and Bittman, R. (2004) The critical micelle concentrations of lysophosphatidic acid and sphingosylphosphorylcholine. *Chem. Phys. Lipids* 130, 197–201.
35. Radford, S. E., Gosal, W. S., and Platt, G. W. (2005) Towards an understanding of the structural molecular mechanism of beta(2)-microglobulin amyloid formation in vitro. *Biochim. Biophys. Acta* 1753, 51–63.
36. Sreerama, N., and Woody, R. W. (1993) A self-consistent method for the analysis of protein secondary structure from circular-dichroism. *Anal. Biochem.* 209, 32–44.
37. Manavalan, P., and Johnson, W. C. Jr. (1987) Variable selection method improves the prediction of protein secondary structure from circular dichroism spectra. *Anal. Biochem.* 167, 76–85.
38. Compton, L. A., and Johnson, W. C. Jr. (1986) Analysis of protein circular dichroism spectra for secondary structure using a simple matrix multiplication. *Anal. Biochem.* 155, 155–167.
39. Provencher, S. W. (1982) Contin—A general-purpose constrained regularization program for inverting noisy linear algebraic and integral-equations. *Comput. Phys. Commun.* 27, 229–242.
40. Provencher, S. W., and Glockner, J. (1981) Estimation of globular protein secondary structure from circular dichroism. *Biochemistry* 20, 33–37.
41. van Stokkum, I. H., Spoelder, H. J., Bloemendal, M., van Grondelle, R., and Groen, F. C. (1990) Estimation of protein secondary structure and error analysis from circular dichroism spectra. *Anal. Biochem.* 191, 110–118.
42. Andrade, M. A., Chacon, P., Merelo, J. J., and Moran, F. (1993) Evaluation of secondary structure of proteins from UV circular dichroism spectra using an unsupervised learning neural network. *Protein Eng.* 6, 383–390.
43. Hubbard, S. J. (1998) The structural aspects of limited proteolysis of native proteins. *Biochim. Biophys. Acta* 1382, 191–206.
44. Tanford, C. (1974) Thermodynamics of micelle formation: prediction of micelle size and size distribution. *Proc. Natl. Acad. Sci. U.S.A.* 71, 1811–1815.
45. Iwata, K., Matsuura, T., Sakurai, K., Nakagawa, A., and Goto, Y. (2007) High-resolution crystal structure of beta2-microglobulin formed at pH 7.0. *J. Biochem. (Tokyo)* 142, 413–419.
46. Kardos, J., Yamamoto, K., Hasegawa, K., Naiki, H., and Goto, Y. (2004) Direct measurement of the thermodynamic parameters of amyloid formation by isothermal titration calorimetry. *J. Biol. Chem.* 279, 55308–55314.
47. Chiti, F., De Lorenzi, E., Grossi, S., Mangione, P., Giorgetti, S., Caccialanza, G., Dobson, C. M., Merlini, G., Ramponi, G., and Bellotti, V. (2001) A partially structured species of beta2-microglobulin is significantly populated under physiological conditions and involved in fibrillogenesis. *J. Biol. Chem.* 276, 46714–46721.
48. Eakin, C. M., Berman, A. J., and Miranker, A. D. (2006) A native to amyloidogenic transition regulated by a backbone trigger. *Nat. Struct. Mol. Biol.* 13, 202–208.
49. Horwich, A. (2002) Protein aggregation in disease: a role for folding intermediates forming specific multimeric interactions. *J. Clin. Invest.* 110, 1221–1232.
50. Jahn, T. R., Parker, M. J., Homans, S. W., and Radford, S. E. (2006) Amyloid formation under physiological conditions proceeds via a native-like folding intermediate. *Nat. Struct. Mol. Biol.* 13, 195–201.
51. Kameda, A., Hoshino, M., Higurashi, T., Takahashi, S., Naiki, H., and Goto, Y. (2005) Nuclear magnetic resonance characterization of



- the refolding intermediate of beta2-microglobulin trapped by non-native prolyl peptide bond. *J. Mol. Biol.* 348, 383–397.
52. Uversky, V. N., and Fink, A. L. (2004) Conformational constraints for amyloid fibrillation: the importance of being unfolded. *Biochim. Biophys. Acta* 1698, 131–153.
53. Gorbenko, G. P., and Kinnunen, P. K. (2006) The role of lipid-protein interactions in amyloid-type protein fibril formation. *Chem. Phys. Lipids* 141, 72–82.
54. Gellermann, G. P., Appel, T. R., Tannert, A., Radestock, A., Hortschansky, P., Schroeckh, V., Leisner, C., Lutkepohl, T., Shtrasburg, S., Rocken, C., Pras, M., Linke, R. P., Diekmann, S., and Fandrich, M. (2005) Raft lipids as common components of human extracellular amyloid fibrils. *Proc. Natl. Acad. Sci. U.S.A.* 102, 6297–6302.
55. Hagihara, Y., Hong, D. P., Hoshino, M., Enjyoji, K., Kato, H., and Goto, Y. (2002) Aggregation of beta(2)-glycoprotein I induced by sodium lauryl sulfate and lysophospholipids. *Biochemistry* 41, 1020–1026.
56. Floege, J., and Ehlerding, G. (1996) Beta-2-microglobulin-associated amyloidosis. *Nephron* 72, 9–26.
57. Koch, K. M. (1992) Dialysis-related amyloidosis. *Kidney Int.* 41, 1416–1429.
58. Yamaguchi, K., Naiki, H., and Goto, Y. (2006) Mechanism by which the amyloid-like fibrils of a beta2-microglobulin fragment are induced by fluorine-substituted alcohols. *J. Mol. Biol.* 363, 279–288.
59. Calabrese, M. F., Eakin, C. M., Wang, J. M., and Miranker, A. D. (2008) A regulatable switch mediates self-association in an immunoglobulin fold. *Nat. Struct. Mol. Biol.* 15, 965–971.
60. Jahn, T. R., Tennent, G. A., and Radford, S. E. (2008) A common beta-sheet architecture underlies in vitro and in vivo beta2-microglobulin amyloid fibrils. *J. Biol. Chem.* 283, 17279–17286.
61. Meleh, M., Pozlep, B., Mlakar, A., Meden-Vrtovec, H., and Zupancic-Kralj, L. (2007) Determination of serum lysophosphatidic acid as a potential biomarker for ovarian cancer. *J. Chromatogr., B: Anal. Technol. Biomed. Life Sci.* 858, 287–291.
62. Sasagawa, T., Suzuki, K., Shiota, T., Kondo, T., and Okita, M. (1998) The significance of plasma lysophospholipids in patients with renal failure on hemodialysis. *J. Nutr. Sci. Vitaminol. (Tokyo)* 44, 809–818.
63. Sirolli, V., Ballone, E., Di Stante, S., Amoroso, L., and Bonomini, M. (2002) Cell activation and cellular-cellular interactions during hemodialysis: effect of dialyzer membrane. *Int. J. Artif. Organs* 25, 529–537.
64. Thijs, A., Grooteman, M. P., Zweegman, S., Nube, M. J., Huijgens, P. C., and Stehouwer, C. D. (2007) Platelet activation during haemodialysis: comparison of cuprammonium rayon and polysulfone membranes. *Blood Purif.* 25, 389–394.
65. Sano, T., Baker, D., Virag, T., Wada, A., Yatomi, Y., Kobayashi, T., Igarashi, Y., and Tigyi, G. (2002) Multiple mechanisms linked to platelet activation result in lysophosphatidic acid and sphingosine 1-phosphate generation in blood. *J. Biol. Chem.* 277, 21197–21206.